Microelectronics Reliability 145 (2023) 114994

Contents lists available at ScienceDirect

Microelectronics Reliability

journal homepage: www.elsevier.com/locate/microrel

Enhanced solder fatigue life of chip resistor by optimizing solder shape

Jonghwan Ha *, Yangyang Lai, Junbo Yang, Pengcheng Yin, Seungbae Park

Department of Mechanical Engineering, The State University of New York at Binghamton, Binghamton, United States of America

ARTICLE INFO

Keywords:
Fatigue life
Thermal shock
Stencil
Solder shape
Solder volume
Chip resistor
Passive component
Surface Evolver
Darveaux model

ABSTRACT

As surface-mounted components get smaller, especially passive components such as chip resistor or chip capacitor, small apertures on a stencil are required, which generates higher variations in the printed solder paste volume and solder joint shape. In this study, the board-level fatigue life of chip resistor assemblies with SAC305 was investigated. Different volumes of solder paste are printed, which varies the shape of solder joints. Four solder joint shapes are compared: concave, straight, tiny convex, and convex, which are achieved using a stencil with differently sized openings. Thermal shock cycling shows that the convex shape exhibits the best thermal shock reliability while the concave shape has the shortest fatigue life. Additionally, different sizes of chip resistor package are compared. A comparison of the size of components concludes that the R0402 chip resistor has relatively better thermal shock resistance than the larger chip resistor, R1005 due to larger change in length of R1005 during thermal cycling. Based on the experimental results of fatigue life, the parameters of a constitutive equation are calculated to evaluate the fatigue life of the solder joint. This study provides criteria manufacturers can use to improve the reliability of chip assemblies though inspecting solder paste volumes and shapes.

1. Introduction

Chip resistor packages are widely used in surface mount manufacturing. End customer demand for ever smaller handheld devices means chip resistors must continuously get smaller. The trend constantly getting size of chip resistors smaller leads to required also smaller apertures on a stencil, and it tends to generate higher variations in solder paste volume during the typical process of assembling package which is printing solder paste using a given thickness stencil. The variations in solder paste volume induce variations of solder joint shape during reflow. The variations in solder joint shape generate variations in the thermal fatigue life of solder joints, a major cause of failures.

In previous studies, researchers have investigated the formation of solder joints. Theoretically, the final shape of the molten solder occurs in a way that minimizes the energy needed to maintain the shape. The equilibrium shape of molten solder using energy minimization is given by the energy in surface tension and gravity [1–6]. The surface tension energy accounts for the boundaries of solid, liquid, and gaseous phase: solder and gas, solder and pad, and solder and component end termination [7,8]. From the solder paste volume perspective, controlling solder paste volume allows for forming the desired shape on the fillet geometry of the solder joint on the two end terminations of passive components [9]. Furthermore, researchers found that the solder paste volume can significantly affect the standoff height, which is the thickness between copper pad and component termination [10]. The standoff height effectively increases with solder paste volume and it induces higher fatigue life [11,12]. Solder paste volume is not the only geometric factor determining the solder joint shape; the dimensions of the copper pad affect the formation of solder shape in a given size of component [13].

Research has been conducted to predict the fatigue life of solder joints in electronic packages by performing temperature cycling. The mismatch of thermal expansion between the component and PCB can cause cracks to appear during thermal cycling, which then propagate through the fillet of the solder joint. Microstructure of SAC 305 solder joint in chip resistor was investigated. The crack initiates on the underneath where a high strain region associated with local recrystallization and crack propagation is triggered by a significant increase in the recrystallized grains. Crack growth dominates the fatigue life of solder joint in chip resistor since crack initiation denotes less than 15 % of life and it is controlled by recrystallization and IMC coalescence [14,15]. Meantime, the investigation found that the lower standoff height will bring more shear stress resulting in lower shear strength [16]. Adding more solder paste extends the fatigue life against thermal loading [17]. In the same manner, a convex shape on the fillet solder joint generated by adding more solder paste creates longer fatigue life than concave or

* Corresponding author.
E-mail address: jha16@binghamton.edu (J. Ha).

https://doi.org/10.1016/j.microrel.2023.114994
Received 27 December 2022; Received in revised form 13 April 2023; Accepted 14 April 2023
Available online 28 April 2023

tiny concave shapes from smaller amounts of solder paste. However, aside from them, other studies found that tiny concave shapes on the fillet have a longer fatigue life [18]. However, those studies into the correlations between fillet shape and fatigue life took numerical approaches. Experimental studies showed that faster crack growth occurs with larger components, and it causes lower thermal reliability. The study, which investigates failures in chip resistor through finite element analysis, concludes that the fatigue life of solder joint varies tremendously depending on the size of component and the solder joint area also [19].

In this study, four types of solder joint shapes: concave, straight, tiny convex, and convex, are assembled to elucidate the reliability of solder joints depending on the shapes. Test boards are mounted with two types of chip resistors: R1005 and R0402 with SAC305 to analyze the effect of component size. During operating an electronic device, the solder joints experience temperature changes continuously and cyclic thermal loading eventually causes the failure of solder joints from the mismatch of thermal expansions. The investigation for thermal fatigue of solder joints on the resistor package can be done experimentally but the approach is very time-consuming. For this reason, thermal shock cycling tests are often carried out as test method for an extreme environment in the thermal fatigue experiment [20,21]. This study models the extremely harsh condition of thermal shock cycling as a method to reduce time introducing failures in solder joints for chip resistor packages.

2. Experiment setup

Two types of components with different sizes and corresponding pads are selected. The specs of these components are listed in Table 1. To assemble the SAC305 packages, we used the stencil printing method where solder paste is printed through the openings on a given thickness of a stencil. As shown in Fig. 1, the stencil is designed to have four opening sizes that generate the four pre-determined shapes. In a typical group of resistors on one board each will have either a concave, straight, tiny convex, or convex solder joint shape. Components such as R0402 have relatively very small sizes, which means the opening needed to produce the concave shape is also very small. Thus, the stencil opening shape for concave solder joints for R0402 components is designed as a circle instead of a rectangle with rounded corners as with the other shapes. After printing the solder paste, an inspection (SPI) is performed to ensure that the solder pastes on each pad are printed according to their opening size. If there is not enough solder printed, the pastes are removed and the process is repeated until the proper amount is printed.

2.1. Pre-determined solder joint shape in surface evolver

In surface mounted technology, molten solder solidifies into its final shape based on the minimum amount of energy derived from surface tension and gravitational potential energy, hydrostatic and capillary pressure within given constrains such as component termination length, component and pad sizes during reflow soldering [22]. As discussed, thermal fatigue of a solder joint is closely related to its shape and the shape is very dependent on solder paste volume and the geometry of the component and pad. Therefore, optimizing the geometry of the solder joint is an efficient approach to determine the shape of the solder joint

Table 1
Specs of components mounted on boards and pads.

Item	R1005	R0402
Number of components	1320	1320
Length (mm)	0.973	0.401
Height (mm)	0.350	0.153
Width (mm)	0.500	0.200
Termination length (mm)	0.225	0.160

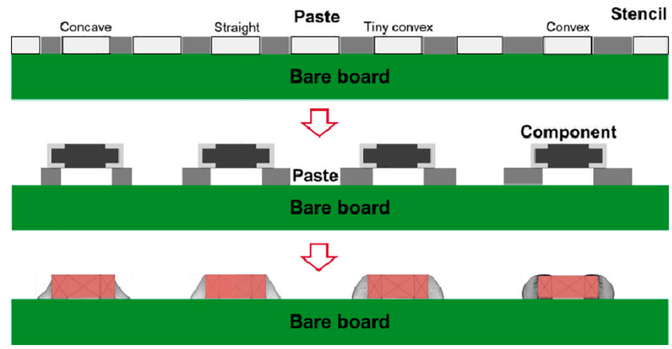

Fig. 1. Assembling process of chip resistor package.

and the thermal reliability of a chip resistor assembly. Surface Evolver allows the study of the behavior or molten solder and calculates the user-defined surface to minimize the energy of a surface [23].

A three-dimensional model of a chip resistor assembly is created in Surface Evolver, and it is validated compared with the cross-sectional samples. Fig. 2 is the Surface Evolver model and Fig. 3 compares the Surface Evolver model and cross-sectional samples.

The standoff height in the chip resistor assembly must be determined precisely because the solder joint underneath the component fails first, and its thermal reliability decreases as standoff height decreases. Reliability lessens as shorter standoff height increase the CTE mismatch. The chip resistor is halted at a certain height itself by the equilibrium state of molten solder depending on the amount of solder paste. Fig. 4 shows the standoff height of cross-sectional samples and model in Surface Evolver.

After validating the model in Surface Evolver, 30 volumes are applied to find typical four volumes of solder paste inducing four pre-determined solder joint shapes. The variations of pre-determined solder joint shape in Surface Evolver are shown in Fig. 5.

The typical process to print solder paste on the pads is one of the most important processes in this study. Stencil is properly aligned under the PCB and the solder paste is deposited on the pads through openings on the stencil by squeegee blade. Then, stencil is removed for pick and placement process. In the process of removing stencil, the portion of solder paste is commonly hold on the sidewalls of stencil opening regarding opening shape. Stencil thickness with respect to size of opening is also taken into the consideration. Since solder volumes for R1005 and R0402 chip resistors are already pre-determined, sizes of stencil opening are changed with regarding thickness of stencil. Thus, opening shape on stencil regarding corner ratio, thickness, and opening distance should be considered to predict proper solder shapes. In order to design the stencil satisfying R1005 convex shape, which is the largest volume and concave shape of R0402 with the smallest volume through one stencil, the stencil is manufactured with an electroformed process that has the largest opening size with stencil thickness of 0.07112 mm. Using the solder volumes inducing concave, straight, tiny convex, and convex from Surface Evolver model and given thickness of stencil, the opening areas satisfying four pre-determined solder shapes are calculated reversely. The length of each opening is determined 10 % smaller than width and corner ratio is defined 50 % to avoid void and deposit solder paste efficiently during printing solder paste. However, corner ratio of opening for R0402 concave shape is defined as 100 % which is shaped as circle due to smaller solder volume with aspect ratio required while opening areas for others are shaped rectangle with rounded corners as shown in Fig. 6 and 7. Corresponding volumes and opening sizes on stencil in Table 2.

2.2. Test vehicle configurations

Rectangular chip resistors R1005 (1.0 × 0.5 mm) and R0402 (0.4 × 0.2 mm), tin finish on nickel, are mounted on a 265 × 215 × 1.6 mm FR-

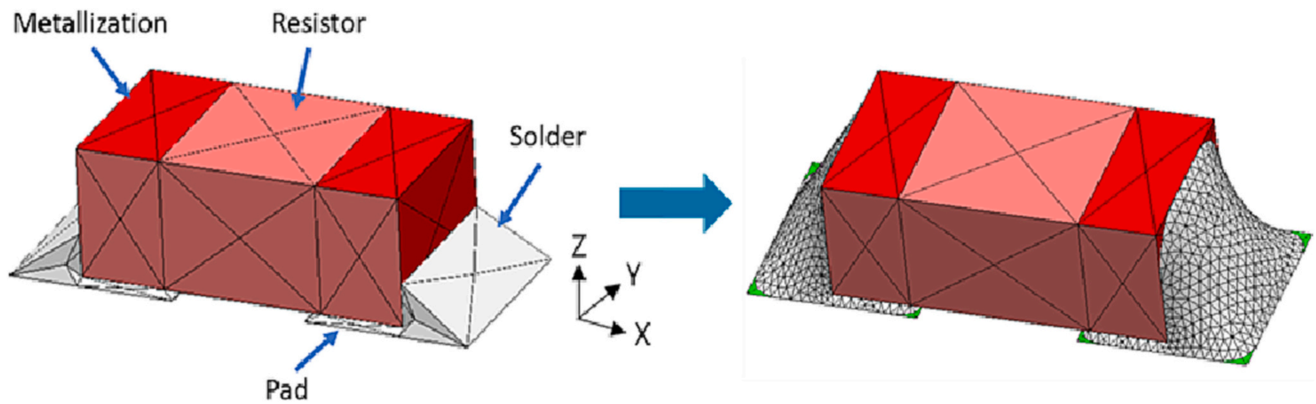

Fig. 2. Model of chip resistor assembly in Surface Evolver.

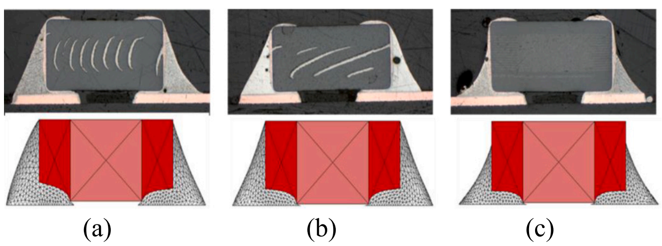

Fig. 3. Comparison of Surface Evolver model and samples (a) 139–103 % (b) 102–164 % (c) 66–69 % solder volume.

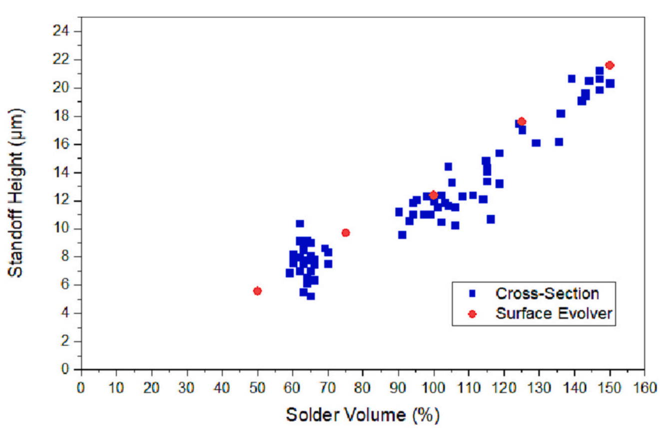

Fig. 4. Standoff height of samples and model in Surface Evolver.

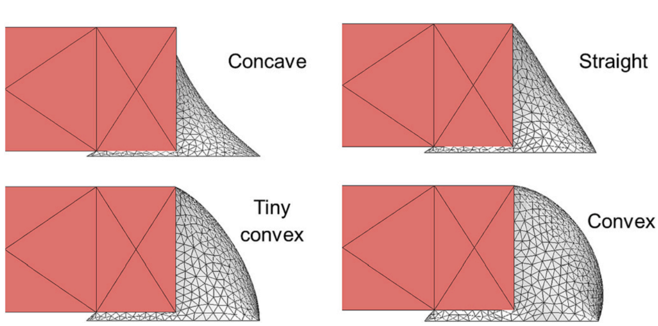

Fig. 5. Pre-determined solder shapes in Surface Evolver.

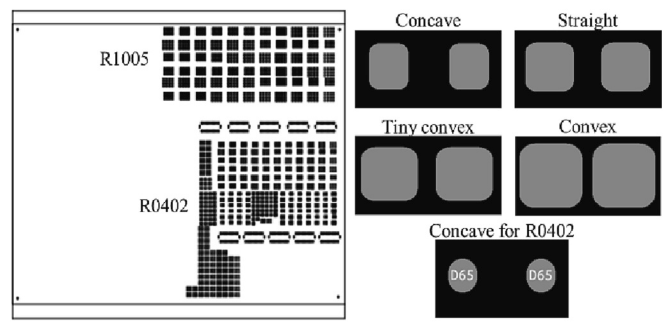

Fig. 6. Stencil design and openings.

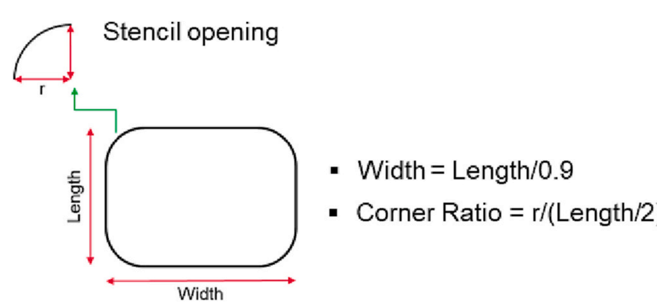

Fig. 7. Stencil opening determination.

Table 2
Stencil opening area and volume.

Component type	Solder shape	Opening area (mm^2)	Volume (mm^3)
R0402	Concave	0.015529	0.001104
	Straight	0.025880	0.001841
	Tiny convex	0.036233	0.002577
	Convex	0.046585	0.003313
R1005	Concave	0.233857	0.016632
	Straight	0.389651	0.027712
	Tiny convex	0.545667	0.038808
	Convex	0.701572	0.049896

4 PCB. SAC 305 (Sn3.0Ag0.5Cu) solder is employed to mount the components on the electroless nickel immersion gold (ENIG) copper pads. Through the uniquely designed stencil, which has different opening areas for each column on the PCB, six groups of chip resistors are assembled to have the same shape of solder joint to evaluate the reliability of variations in solder shape. The shape of the solder joint composed of concave in the first column, straight in the second, tiny

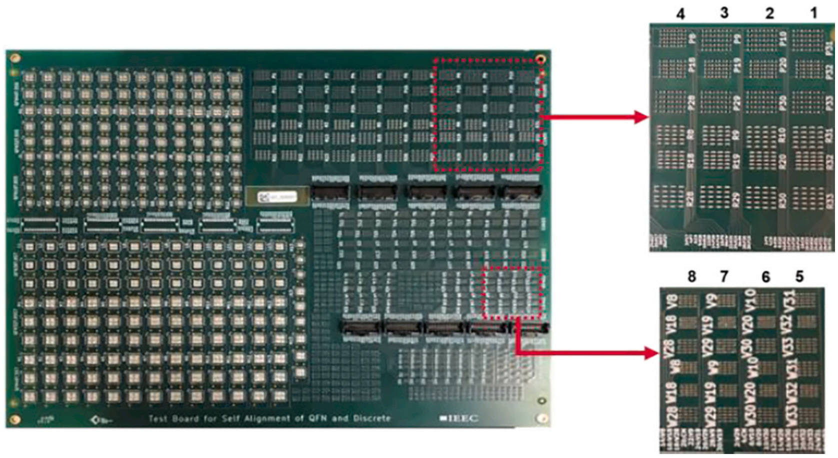

Fig. 8. Board layout of solder shape variations.

Table 3
Details of solder shape variations in board.

Number	Component type	Solder shape	Condition
1	R1005	Concave	Symmetry
2		Straight	
3		Tiny convex	
4		Convex	
5	R0402	Concave	
6		Straight	
7		Tiny convex	
8		Convex	

convex in the third, and convex in the fourth as shown in Fig. 8 and the details are in Table 3. Also, the images of printed solder paste for typical shape conditions are shown in Fig. 9. Reflow soldering is conducted using six zones oven under reflow recommendation profile [24,25].

To represent thermal fatigue test in a harsh environment such as aerospace or automotive application, thermal shock test is conducted under the condition: -55 to 150 °C respectively with 3-minute dwell and 2-minute ramp time based on the standards, JESD22-A106 and IEC-60068, which can be seen in Fig. 10 [26–28].

All components and boards are internally daisy-chained to connect the components as shown in Fig. 11. Twenty chip resistors are grouped to connect one channel for inspecting in-situ resistance. Furthermore, six groups of components are created to have the same shaped solder joints. Based on the in-situ measurement of resistance change obtained from connectors, failures of solder joints could be anticipated. In this experiment, hard open, which is the infinite value of resistance, is adopted as the failure criterion instead of a 20% resistance increase from an initial value or resistance exceeding a threshold as there is possibility that a crack occurs with no significant change of resistance if the initial resistance of the resistor is relatively high [29,30].

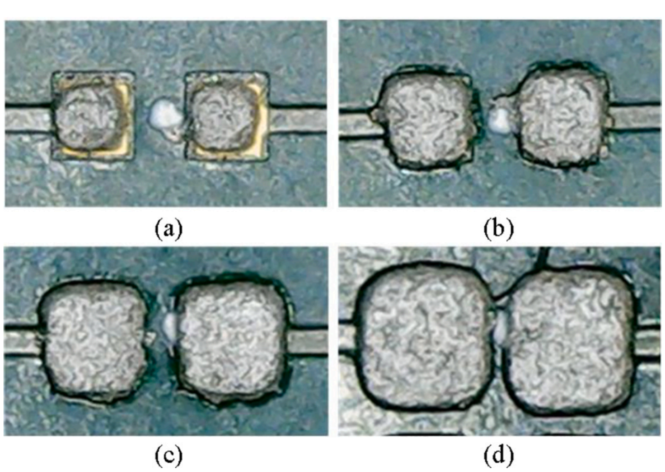

Fig. 9. Printed solder pastes of shape variations (a) concave (b) straight (c) tiny convex (d) convex.

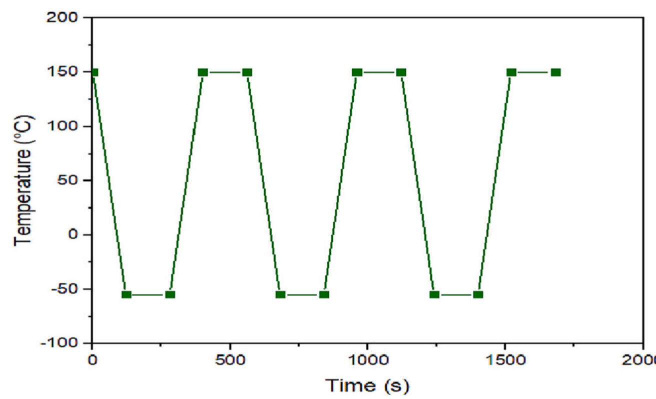

Fig. 10. Temperature profile for a thermal shock cycling test.

3. Results and discussion

3.1. Fatigue test experiment results

Figs. 12 and 13 show the Weibull plot of the test results for four solder shape conditions for each type of resistor. Among the variations in solder shape, the convex shape shows the most reliability with a characteristic time to failure (TTF, 63.2%) of 14,183 cycles; the tiny convex shape comes in second with TTF of 12,724 cycles; the straight shape in third with TTF 11737 cycles; and concave shape shows the most failures with TTF 10873 cycles. According to the result, it is concluded that the convex shape, which is the largest solder volume usually has approximately 30% higher fatigue life than concave shape; tiny convex shape comes in next with a 17% increase; convex shape solder fatigue life in third with 7.9 % higher than that of the concave shape solder; and the concave shape, which is the smallest solder volume will fail earlier as shown in Table 4. Larger solder volume increases standoff height, which is the thickness between component termination and pad and it induces longer fatigue life on standoff height. Moreover, it needs longer time to emerge crack on the surface of fillet as larger solder volume is formatted on the fillet [31]. Overall, adding more solder volume induces longer fatigue life of both underneath and fillet so that total fatigue life also

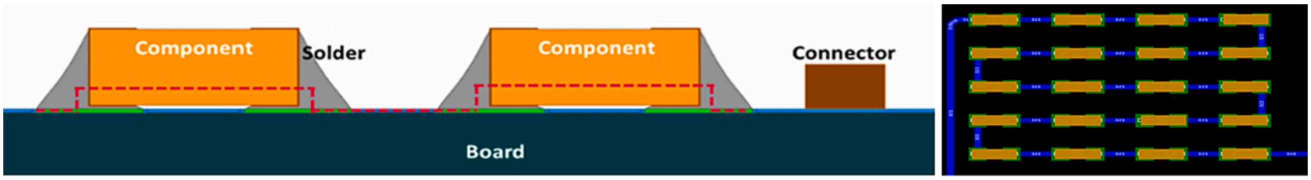

Fig. 11. Daisy chained structure of PCB and chip resistors.

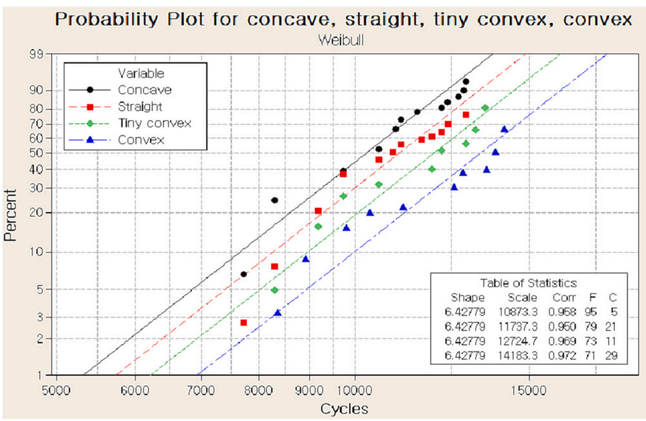

Fig. 12. Weibull plot of thermal shock cycling result of R1005.

increases.

To understand the cracking in the solder joint, chip resistors are cross-sectioned as shown in Fig. 14. The cracks in the most samples propagated along the boundaries of resistor termination. This is the typical crack route induced when the solders undergo thermal shock loading. Thermal shock cycling involves rapid and sudden temperature changes, and the faster rate of temperature changes induces cracks near the termination of the component instead of cracks along the middle of the fillet in the solder joint [32]. In this manner, fatigue is more sensitive to CTE mismatch between solder and component, which influences the crack route more than the CTE mismatch between solder and substrate [33].

3.2. Fatigue life of actual volume in solder joint

In SMT, solder paste is printed through openings on a stencil. The paste may not be printed properly and smaller or larger amounts than intended will be deposited through the stencil opening. Therefore, the exact volume of solder needed for an intended shape to be reliable may not be deposited. Fig. 15 shows the thermal shock cycles by actual volumes measured by the solder paste inspection (SPI) machine of each pre-determined shape. 100% of the solder volumes of each case means solder paste is printed correctly. In the micro view of fatigue life, the fatigue life is increased proportionally depending on the solder paste volumes as agree with previous results.

3.3. Development of life prediction model

Among many models of life prediction such as Steinberg's stress based [34], Engelmaier's strain based [35], and Darveaux's energy-based [36] approaches, Darveaux's model is commonly employed for modeling [37]. In this study, Darveaux's model with the Anand model, which represents the constitutive behavior of solder material is adapted. The

Table 4
Time to failures 63.2% of solder shapes.

Component	Solder shape	TTF 63.2 %	% increase
R1005	Concave	10,873	
	Straight	11,737	7.9
	Tiny convex	12,724	17
	Convex	14,183	30
R0402	Concave	12,728	
	Straight	13,508	6.1
	Tiny convex	15,077	19
	Convex	17,572	38

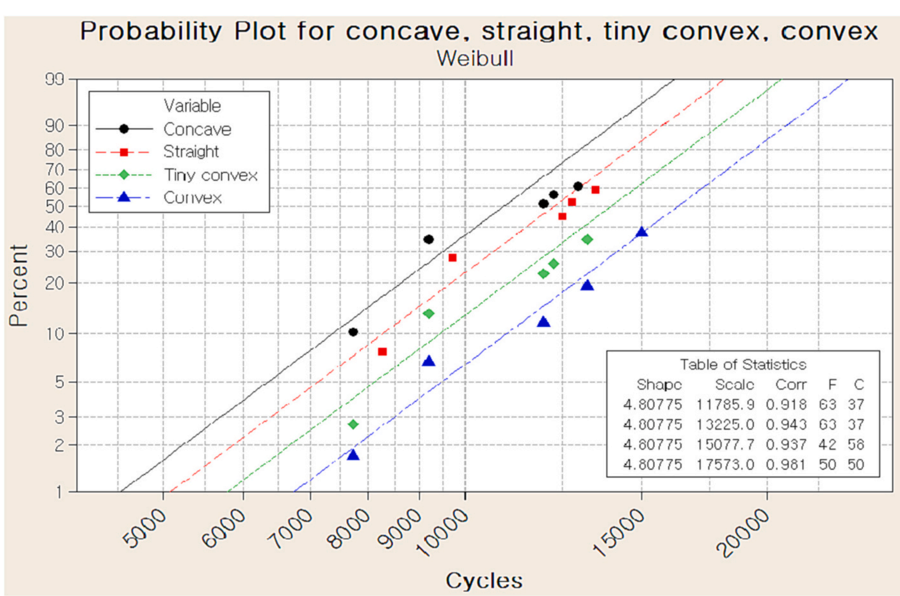

Fig. 13. Weibull plot of thermal shock cycling result of R0402.

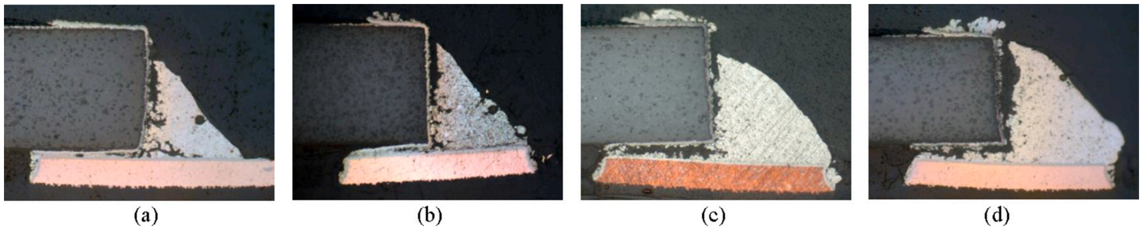

Fig. 14. SAC305 solder joint images representative thermal shock fatigue failures (a) concave (b) straight (c) tiny convex (d) convex.

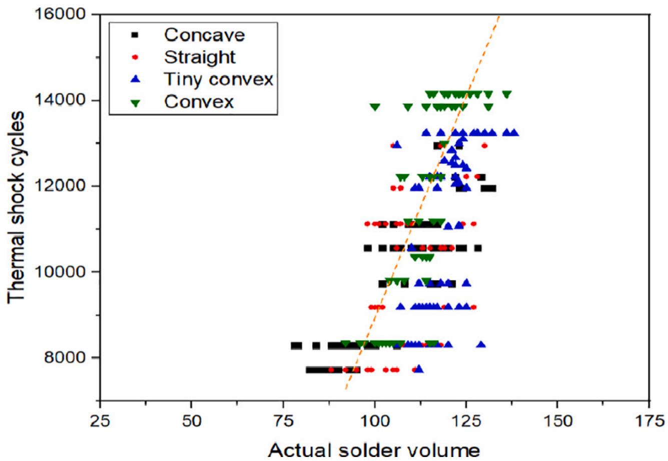

Fig. 15. Results of thermal shock cycles versus actual volume.

Table 5
Constants of ANAND model for SAC305 [38].

Parameter	Definition	Value
s_0 (MPa)	Initial value of deformation resistance	2.15
Q/k (K)	Activation energy of solder/Boltzmann's constant	9970
A (1/s)	Pre-exponential factor	17.994
ξ (dimensionless)	Multiplier of stress	0.35
m (dimensionless)	Strain rate sensitivity of stress	0.153
h_0 (MPa)	Hardening constant	1526
$\hat{s}$ (MPa)	Coefficient for deformation resistance saturation value	2.536
n (dimensionless)	Strain rate sensitivity of saturation value	0.028
a (dimensionless)	Strain rate sensitivity of hardening	1.69

constants of SAC305 in the Anand model are listed in Table 5 [38].

$$\frac{d\varepsilon_p}{dt} = A[sinh(\xi\sigma/s)]^{1/m}exp\left(\frac{-Q}{kT}\right) \tag{1}$$

$$\frac{ds}{dt} = \left\{h_0(|B|)^a\frac{B}{|B|}\right\}\frac{d\varepsilon_p}{dt} \tag{2}$$

$$B = 1 - \frac{s}{s^*} \tag{3}$$

$$s^* = \hat{s}\left[\frac{d\varepsilon_p/dt}{A}\right]exp\left(\frac{Q}{kT}\right)^n \tag{4}$$

According to the constants of the constitutive equations, a finite element model is utilized to analyze the inelastic strain energy density accumulated per each thermal cycle inside the solder joints and determine the fatigue life depending on the solder shapes. To build a more realistic FEA model, the geometry of the model in Surface Evolver is imported into the model as shown in Fig. 16.

The properties of materials in the model are applied as linear elastic solid expect solder alloy as nonlinear. For mesh in finite element analysis, solid 186, which is higher order quadratic element, is selected for chip resistor, PCB, and solder mask, and solid 187 and 186 for pad, termination and solder joint due to complicated geometry.

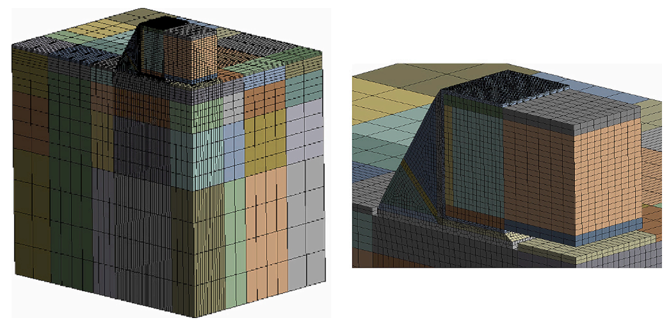

Fig. 16. Meshed FEA model.

To determine minimum mesh size required to produce near mesh independent results and satisfied analysis time, mesh size sensitivity should be confirmed simulating various size of mesh using three mesh models. It is shown that the differences of accumulated energy density between three mesh models are less than 5%. However, time for analysis in mesh 3 model is slightly higher than the others as shown in Table 6. Thus, mesh 2 model is suitable for this parametric study to conduct with efficient computing sources.

The FEA model is separated into two parts to estimate the lifetime of solder joint as shown in Fig. 17. In the first step, the model is simulated including all solder in place for average plastic work in the whole area underneath in solder joint. In the second step, a new model that does not include the underneath area is simulated to calculate the average plastic work in the fillet area and find the possible crack direction (Table 7 and 8).

Since it is assumed that the underneath is already fully disconnected due to the crack). The highest average plastic work indicates the location of high damage and the most likely direction for crack propagation. The locations of the highest average plastic work for four FEA models having four different solder shapes are demonstrated in the 90° directions and the predicted locations of simulations are consistent with experimentally observed locations as shown in Fig. 14.

Darveaux's model predicts of fatigue life based on energy accumulation.

$$N_0 = K_1 \bullet \Delta W_{avg}{}^{K_2} \tag{5}$$

Table 6
Effect of meshing.

		Mesh 1	Mesh 2	Mesh 3
Mesh size (μm)		20	10	5
Acc. energy density (MPa)	Underneath	0.38654	0.38036	0.36922
	Fillet	0.49726	0.48902	0.47404
% diff in acc. energy density	Underneath		1.60	2.93
	Fillet		1.85	3.06
% Diff. in time	Underneath		58	57
	Fillet		22	29

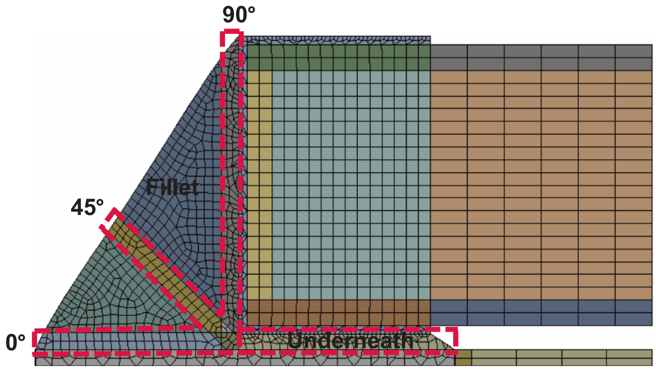

Fig. 17. Possible crack direction on solder joint.

Table 7
Material properties [17].

Materials	Young's modulus (GPa)	Poisson's ratio	CTE (ppm/°C)
Resistor	282.7	0.22	6.67
Termination	83	0.37	18.9
Solder	28–48	0.40	21.7
Copper pad	121	0.34	16.7
PCB	16.5–21.5	0.39	16.5
Solder mask	2.4	0.30	60–160

Table 8
Sample dimensions in simulations.

Materials	Dimensions (mm)
Termination thickness	0.007
Copper pad	0.56 × 0.5 × 0.02
Solder mask thickness	0.02
PCB	3.42 × 2.56 × 1.58

$$\frac{da}{dN} = K_3 \bullet \Delta W_{avg}{}^{K_4} \tag{6}$$

$$\alpha = N_0 + \frac{a}{da/dN} \tag{7}$$

where N_0 is the number of cycles crack initiated, da/dN is crack propagation rate, α is total fatigue life, a is crack length, ΔW_{avg} is accumulated energy density, K_1, K_2, K_3, and K_4 are fatigue model constants. The K constants depend on the material. However, they are often changed depending on the geometry of the package such as the shapes and dimensions of components and solder joints [39,40]. Number of cycles crack initiated, N_0 is negligible for the solder joint in chip resistor due to relatively smaller number, which is less than 10% of the life time, comparing crack propagation [8,15,40,41]. Thus, constants, K_1 and K_2 are not considered in this study and only crack propagation rate is considered to calculate total fatigue life.

The development of energy-based models for four solder shapes appears in Table 9 and Fig. 18. The plastic work decreases as the change of solder shape following concave, straight, tiny convex, and convex. That means that fatigue life is increasing if the solder volume is increasing because of standoff height. The greater thickness of standoff height induces a trend of decreasing maximum stress. Moreover, the interface layer on 90° has the shortest fatigue life because the crack will propagate in the interface layer near the component termination instead of in the interface layer near the pad.

The values of K_3 and K_4 were experimentally obtained by plugging cycles from the test data, Table 4, accumulated energy density from FEA results, and crack length, Table 9 into Eq. (8), and fitting equations. The constants are presented in Table 10.

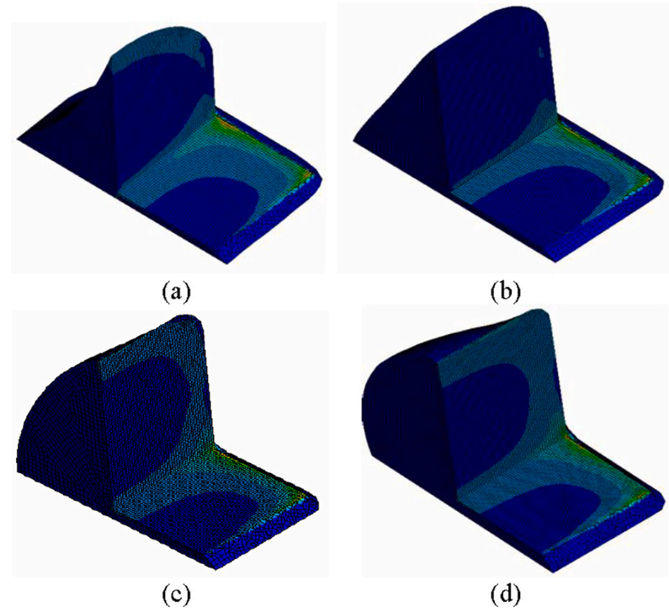

Fig. 18. Energy distribution in sectional image of quarter symmetric model (a) concave (b) straight (c) tiny convex (d) convex.

Table 9
Plastic work results of simulation.

Solder shape	Underneath		Fillet	
	ΔW_{avg} (MPa)	a (μm)	ΔW_{avg}	a
Concave	0.39059	240	0.41405	264
Straight	0.38036	240	0.48902	347
Tiny convex	0.33932	240	0.45263	357
Convex	0.27534	240	0.42584	364

Table 10
K constant values of DARVEAUX model.

Constant	K_3 (μm/cycle • MPa^{K_4})	K_4
Value	0.0827	0.6183

Table 11
Plastic Work Results of Simulation.

Solder shape	Experimental	FEA	% difference
	N_f	N_f	
Concave	10,873	10,696	4.65
Straight	11,737	11,806	0.58
Tiny convex	12,724	12,701	0.18
Convex	14,183	13,904	2.01

$$\alpha_{total} = \alpha_{underneath} + \alpha_{fillet} = \frac{a_1}{K_3 \bullet \Delta W_{avg1}{}^{K_4}} + \frac{a_2}{K_3 \bullet \Delta W_{avg2}{}^{K_4}} \tag{8}$$

where a_1 and a_2 are the crack length of underneath and fillet in solder joint and $\Delta W_{avg,1}$ and $\Delta W_{avg,2}$ are the accumulated energy density in underneath and fillet in solder joint.

The comparison between the measured and predicted lifetimes of thermal shock cycling appears in Table 11. In most cases, it is observed that good agreement is obtained.

4. Conclusion

In this study, two sizes of chip resistors, R1005 and R0402, are assembled with SAC305 based on a stencil that has four different openings areas. Four solder volumes are printed on a board so that four solder shapes, concave, straight, tiny convex, and convex induced by different solder volumes of chip resistor assemblies are compared under the thermal shock cycling. Based on the results of thermal shock cycling, the convex solder joint shows the best thermal shock resistance, tiny convex the second, straight the third, and concave shape has the shortest fatigue life. Fatigue life increase if the solder volume increase in the underneath and fillet areas. The failure mechanism is investigated through the cross-sectional images. The crack is initiated underneath the component and propagates along the path near the component termination instead of near the pad.

The model of finite element analysis is performed in the same thermal shock cycling and constitutive equation and constants for Darveaux's model are determined. Therefore, the fatigue life of a chip resistor with SAC305 assemblies can be predicted by finite element analysis. The results of FEA show good agreement with the experimental results.

CRediT authorship contribution statement

Jonghwan Ha: Conceptualization, Methodology, Software, Formal analysis, Investigation, Writing – original draft. **Yangyang Lai:** Data curation, Resources. **Junbo Yang:** Validation, Investigation. **Pengcheng Yin:** Formal analysis, Software. **Seungbae Park:** Resources, Supervision, Writing – review & editing, Funding acquisition.

Declaration of competing interest

The authors declare that they have no known competing financial interests or personal relationships that could have appeared to influence the work reported in this paper.

Data availability

The authors do not have permission to share data.

References

[1] G. Subbarayan, Y. Li, R.L. Mahajan, Reliability Simulations for Solder Joints Using Stochastic Finite Element and Artificial Neural Network Models, 1996.
[2] G. Subbarayan, A Procedure for Automated Shape and Life Prediction in Flip-chip and BGA Solder Joints, 1996.
[3] A.M. Deshpande, G. Subbarayan, R.L. Mahajan, Maximizing Solder Joint Reliability Through Optimal Shape Design, 1997.
[4] G. Subbarayan, A. Deshpande, The Nature of Centroidal Locus in Misaligned Flip-chip Solder Joints, 1997.
[5] Y. Li, R.L. Mahajan, G. Subbarayan, The Effect of Stencil Printing Optimization on Reliability of CBGA and PBGA Solder Joints, 1998.
[6] D. Kulkarni, G. Subbarayan, A dynamic model for predicting the motion of solder droplets during assembly, in: ITHERM 2000. The Seventh Intersociety Conference on Thermal and Thermomechanical Phenomena in Electronic Systems (Cat. No. 00CH37069) Vol. 1, IEEE, 2000, May, pp. 368–376.
[7] O. Krammer, Modelling the self-alignment of passive chip components during reflow soldering, Microelectron. Reliab. 54 (2) (2014) 457–463.
[8] C. Cai, J. Xu, H. Wang, S.B. Park, A comparative study of thermal fatigue life of eutectic sn-bi, hybrid sn-Bi/SAC and SAC solder alloy BGAs, Microelectron. Reliab. 119 (2021), 114065.
[9] S.M. Heinrich, P.E. Liedtke, N.J. Nigro, A.F. Elkouh, P.S. Lee, Effect of chip and pad geometry on solder joint formation in SMT, J. Electron. Packag. Trans. ASME 115 (4) (1993) 433–439.
[10] W. Tian, X. Hou, H. Cui, X. Feng, A method of research for the reliability of solder joint shape, in: 2021 22nd International Conference on Electronic Packaging Technology (ICEPT), IEEE, 2021, September, pp. 1–4.
[11] K. Pan, J.H. Ha, H. Wang, J. Xu, S. Park, An analysis of solder joint formation and self-alignment of chip capacitors, IEEE Trans. Compon. Packag. Manuf. Technol. 11 (1) (2020) 161–168.
[12] J. Ha, K. Pan, H. Wang, D.H. Won, S.B. Park, The effect of misaligned passive component on fatigue life of solder joints and solder shape, in: 2020 19th IEEE Intersociety Conference on Thermal and Thermomechanical Phenomena in Electronic Systems (ITherm), IEEE, 2020, July, pp. 1029–1034.
[13] L.S. Goldmann, Geometric optimization of controlled collapse interconnections, IBM J. Res. Dev. 13 (3) (2010) 251–265.
[14] M.E.A. Belhadi X. Wei P. Vyas R. Zhao S.D. Hamasha H. Ali J. Suhling P. Lall B.C. Prorok , Reliability and IMC Layer Evolution of Homogenous Lead-Free Solder Joints During Thermal Cycling.
[15] E.B. Romdhane, P. Roumanille, A. Guédon-Gracia, S. Pin, P. Nguyen, H. Frémont, Early microstructural indicators of crack initiation in lead-free solder joints under thermal cycling, in: 2021 IEEE 71st Electronic Components and Technology Conference (ECTC), IEEE, 2021, June, pp. 2293–2301.
[16] T. Garami, O. Krammer, Investigating the mechanical effect of the solder joint thickness with simulation, in: 2013 IEEE 19th International Symposium for Design and Technology in Electronic Packaging (SIITME), IEEE, 2013, October, pp. 259–262.
[17] H. Wang, K. Pan, J. Ha, C. Cai, J. Xu, S. Park, The effect of solder paste volume on chip resistor solder joint fatigue life, Procedia Manuf. 38 (2019) 1372–1380.
[18] G. Zheng, C. Wang, Shape and fatigue life prediction of chip resistor solder joints, in: 2009 International Conference on Electronic Packaging Technology & High Density Packaging, IEEE, 2009, August, pp. 1167–1170.
[19] M.J. Rizvi, H. Lu, C. Bailey, E. Bevan, N. Pountney, J. Coates, Finite element modelling of failures in thick film chip resistor solder joints, in: 2010 5th International Microsystems Packaging Assembly and Circuits Technology Conference, IEEE, 2010, October, pp. 1–4.
[20] J. Gao, J.B. Kwak, Reliability and thermal fatigue life prediction of solder joints for advanced automotive microelectronics, J. Mech. Sci. Technol. 35 (2021) 3633–3641.
[21] M. Al Ahsan, S.K. Hasan, A. Fahim, J.C. Suhling, P. Lall, Effect of different thermal cycling profiles on the mechanical behavior of SAC305 lead free solder, in: 2020 19th IEEE Intersociety Conference on Thermal and Thermomechanical Phenomena in Electronic Systems (ITherm), IEEE, 2020, July, pp. 1170–1179.
[22] J. Berthier, K.A. Brakke, S. Mermoz, C. Frétigny, L. Di Cioccio, Stabilization of the tilt motion during capillary self-alignment of rectangular chips, Sensors Actuators A Phys. 234 (2015) 180–187.
[23] K.A. Brakke, in: Surface Evolver Manual 2.24, Mathematics Department, Susquehanna Univeristy, Selinsgrove, PA, 17870, 1994, p. 20..
[24] Y. Lai, The optimal solution of reflow oven recipe based on physics- guided machine learning model, in: IEEE Intersociety Conference on Thermal and Thermomechanical Phenomena in Electronic Systems (iTherm), 2022 vol. in press.
[25] Y. Lai, A deep learning approach for reflow profile prediction, in: Proceedings - Electronic Components and Technology Conference vol. 2022-May, 2022, pp. 2269–2274, https://doi.org/10.1109/ECTC51906.2022.00358.
[26] J. Favata, S. Shahbazmohamadi, Realistic non-destructive testing of integrated circuit bond wiring using 3-D X-ray tomography, reverse engineering, and finite element analysis, Microelectron. Reliab. 83 (2018) 91–100.
[27] J.E.D.E.C Standard, Thermal Shock. JESD22-A106-A, 1995.
[28] International Electrotechnical Commission, IEC-60068-2-27: 2008: Environmental Testing—Part 2-27: Tests—Test Ea and Guidance: Shock, 2008.
[29] J. Pan, J. Silk, A study of solder joint failure criteria, in: International Symposium on Microelectronics Vol. 2011, International Microelectronics Assembly and Packaging Society, 2011, January.
[30] J. Pan, A control-chart-based method for solder joint crack detection, J. Microelectron. Electron. Packag. 11 (3) (2014) 94–103.
[31] M. Lederer, A.B. Kotas, G. Khatibi, A lifetime assessment and prediction method for large area solder joints, Microelectron. Reliab. 114 (2020), 113888.
[32] T. Garami, O. Krammer, Investigating micro-alloyed solders with thermal shock tests, in: 2012 IEEE 18th International Symposium for Design and Technology in Electronic Packaging (SIITME), IEEE, 2012, October, pp. 129–132.
[33] M. Dusek, M. Wickham, C. Hunt, The impact of thermal cycling regime on the shear strength of lead-free solder joints, in: Soldering & Surface Mount Technology, 2005.
[34] D.S. Steinberg, Vibration Analysis for Electronic Equipment, 2000.
[35] W. Engelmaier, Fatigue life of leadless chip carrier solder joints during power cycling, IEEE Trans. Components Hybrids Manuf. Technol. 6 (3) (1983) 232–237.
[36] R. Darveaux, Effect of simulation methodology on solder joint crack growth correlation and fatigue life prediction, J. Electron. Packag. 124 (3) (2002) 147–154.
[37] W.W. Lee, L.T. Nguyen, G.S. Selvaduray, Solder joint fatigue models: review and applicability to chip scale packages, Microelectron. Reliab. 40 (2) (2000) 231–244.
[38] K. Rajashekar, Impact of Viscoelastic Material Characterization of PCB's on the Thermomechanical Properties of QFN Thick Package Under Thermal Cycling, The University of Texas at Arlington, 2015.
[39] M.S. Kang, D.S. Kim, Y.E. Shin, The effect of epoxy polymer addition in sn-ag-cu and sn-bi solder joints, Materials 12 (6) (2019) 960.
[40] C. Han, B. Song, Development of life prediction model for lead-free solder at chip resistor, in: 2006 8th Electronics Packaging Technology Conference, IEEE, 2006, December, pp. 781–786.
[41] H.S. Ng, T.Y. Tee, K.Y. Goh, J.E. Luan, T. Reinikainen, E. Hussa, A. Kujala, Absolute and relative fatigue life prediction methodology for virtual qualification and design enhancement of lead-free BGA, in: Proceedings Electronic Components and Technology, 2005. ECTC'05, IEEE, 2005, May, pp. 1282–1291.